

Roughness evolution in ablation of carbon-based materials : multi-scale modelling and material analysis

G.L. Vignoles*, J. Lachaud*, Y. Aspa*[◦]

*Laboratoire des Composites ThermoStructuraux (LCTS)
(UMR 5801 Univ. Bordeaux 1-CNRS-SNECMA-CEA)
3, Allée La Boëtie, Domaine Universitaire, F33600 PESSAC, France

[◦]Institut de Mécanique des Fluides de Toulouse (IMFT)
(UMR 5502 CNRS-INPT-Univ. Paul Sabatier)
Allée Professeur Camille Soula, 31400 TOULOUSE, France

Abstract. Various kinds of carbon-based materials are used for the thermal protection of systems at extreme temperatures, like atmospheric re-entry shields and rocket nozzles, because of their unique ablative properties. A critical issue in the design of such systems is the knowledge of the surface roughness evolution.

This work deals with ablation, either by oxidation or by sublimation, from the material point of view. First, an analysis of the material surfaces by optical and electronic microscopy exhibits various features and scales of roughness morphology : they are presented and classified. Then, a modelling strategy based on the competition between transfer at the material interface and in the overlying bulk phase, with possible reactivity contrasts between the material constituents, is built. Finally, numerical results at various scales are given. The predicted morphologies are in correct agreement with the experimental observations, and allow to identify physico-chemical parameters from the roughness geometry.

INTRODUCTION

Ablative Thermal Protection Systems (TPS) are the most traditional materials for atmospheric re-entry nose-tip protection; among them, carbon/carbon (C/C) and carbon/phenolic resin (C/R) composites are of common use [MAN98, DUF96], because of their excellent compromise between thermal, thermo-chemical and mechanical properties [SAV93]. The principle of thermal protection is that an appreciable amount of the received heat flux is converted into outwards mass flux through endothermic sublimation and chemical etching : this results in surface recession [COU98]. Surface roughening then appears : this banal but uncontrolled phenomenon has several consequences of importance in the case of atmospheric re-entry. First, it increases the chemically active surface of the wall; and second, it contributes to the laminar-to-turbulent transition in the surrounding flow[JAC74,RED79]. Both modifications to the physico-chemistry lead to an increase in heat transfer, resulting in an acceleration of the surface recession [BAT83]. The TPS thickness design has to account for this rather strong effect.

Another spatial application for the same class of materials is the fabrication of rocket nozzle throats and inner parts. Here again, the acquisition of surface roughness during rocket launch is a critical issue, not because of the laminar-to-turbulent transition, but principally because of its impact on surface recession velocity, and on the possibility of triggering mechanical erosion [BOR90].

For both applications, if general phenomenological tendencies are predictable, the understanding of the interaction between the flow and the material has to be improved. In

this work, an effort is done to improve this comprehension through the observation, the study and the modelling of roughness evolution, focusing on the primary cause which is heterogeneous transfer.

This document features three parts:

1. First, a description and a classification of multi-scale surface roughness features appearing on carbon-based materials are proposed;
2. Then, physico-chemical models are set up to explain the formation of the typical roughness patterns;
3. Numerical and analytical results are presented and discussed with respect to the experimental observations.

1. ROUGHNESS DESCRIPTION AND CLASSIFICATION

1.1. Material, tests and observation conditions

The studied material is a 3D C/C composite, made from a 3D ex-PAN carbon fibre preform and a pitch-based carbon matrix. It is a heterogeneous multi-scale material. Several thousands of fibers are linked together into a unidirectional bundle with a pitch-based matrix (mesostructure). Then, bundles are orthogonally fit together into a pattern repeated by translation on a cubic lattice. This macro-structure leads to a network of parallelepipedic macro-pores (located near each node of the lattice), which are partially filled with pitch matrix.

Unfortunately, it is quite difficult to recover samples from real flight experiments. As far as roughness is concerned, arc-jet ground tests are supposed to be representative of real flight conditions [WOO75]. The samples have been submitted to arc-jet tests in stagnation point configuration. The material temperature was high enough (3000 K) to enable both oxidation and sublimation. However, the efficient 3D C/C structure prevents the sample from being notably eroded during ablation.

Other tests have been performed in an atmospheric pressure oxidation reactor, with temperatures ranging from 600 K to 900 K.

Surface roughness has been observed by binocular magnifier (BM), optical microscope (OM), and scanning electron microscopy (SEM).

1.2. Description and classification

A classification of the observed roughness features according to their length scales is presented on Fig. 1.

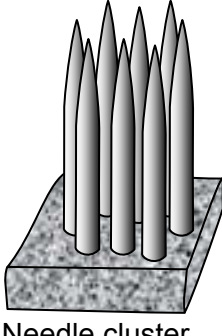
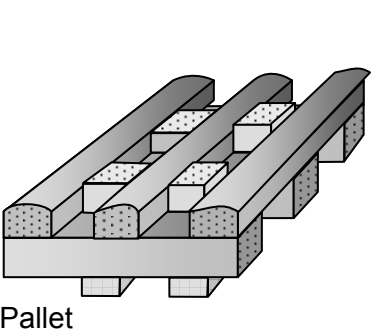
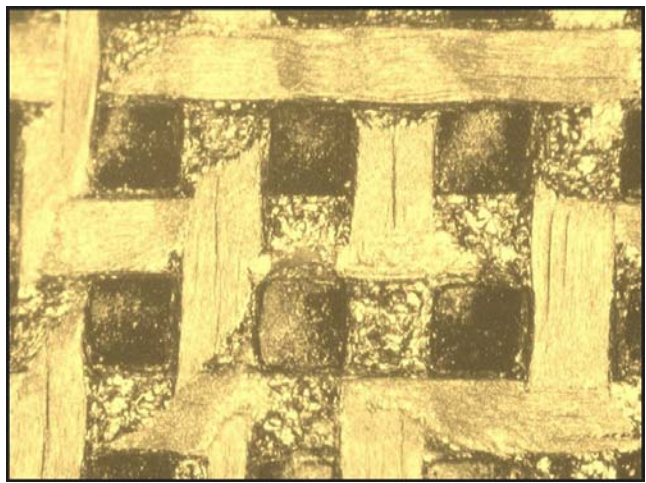
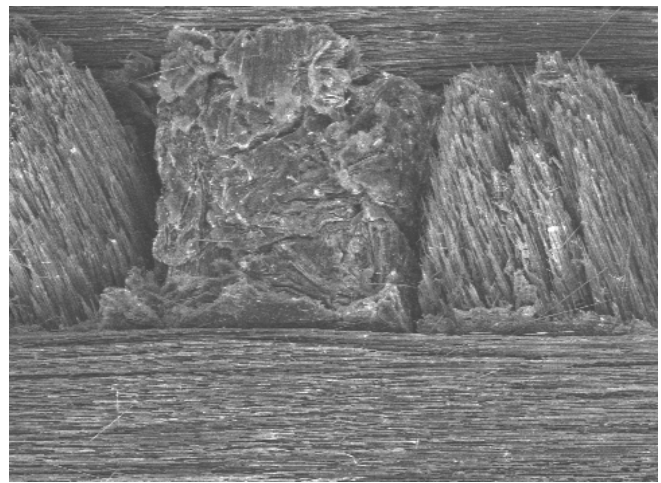
Structural feature	Microstructure	Mesostructure	Macrostructure
Dimensions	Micrometer		Centimeter
Scheme	 Faceted tip with top hole	 Needle cluster	 Pallet
Roughness	Epimicrostructural	Epimesostructural	Epimacrostructural

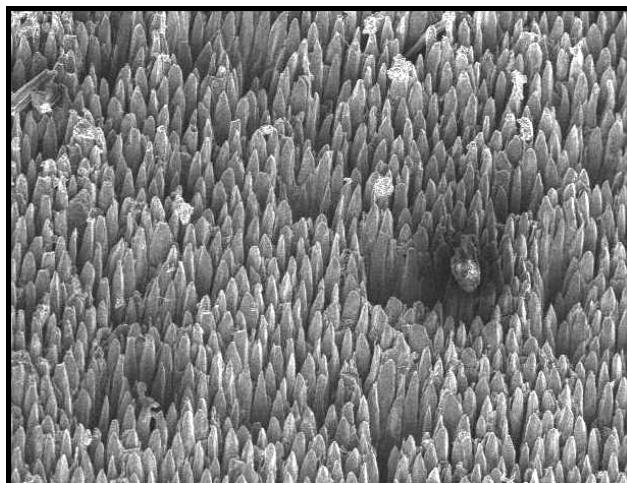
Figure 1 : Summary of roughness features, based on material structural organisation.



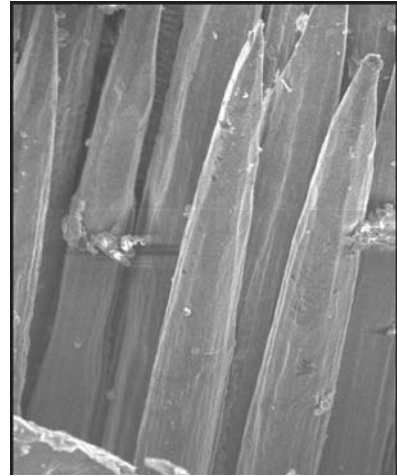
a) Epimacrostructural (BM)



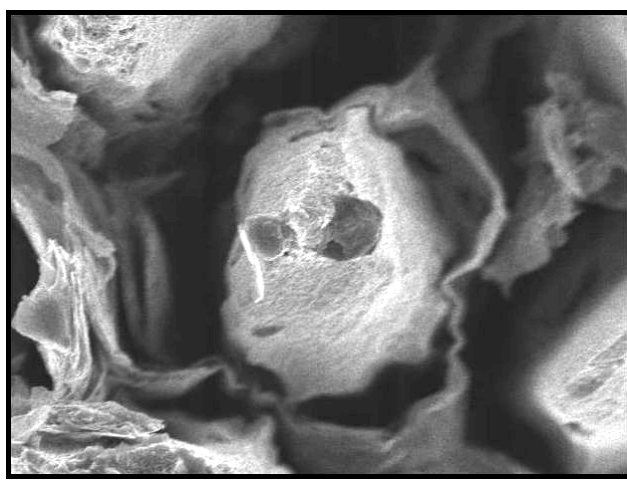
b) Epimacrostructural (SEM)



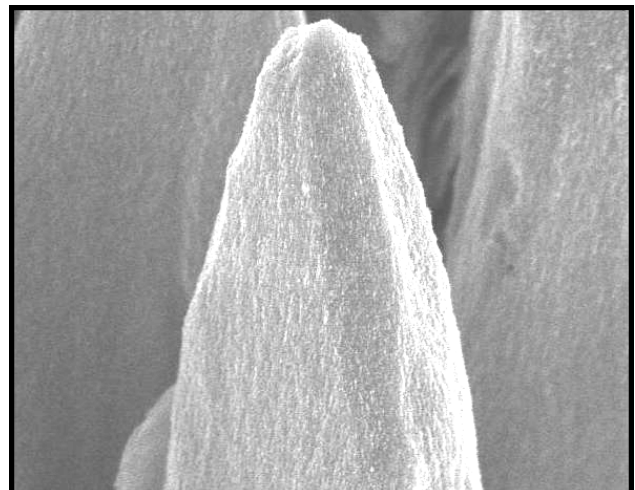
c) Epimesostructural (SEM)



d) Epimesostructural (SEM)



e) Epimicrostructural (SEM)



f) Epimicrostructural (SEM)

Figure 2: Micrographs of 3D C/C surface roughness features after ablation.

For each scale, a sketch and a name are given:

1. *Epimacrostructural* roughness takes place on the lattice. It seems to result from the difference of reactivity between bundles and extra-bundle pitch-based matrix. Mechanical erosion sporadically occurs through the detachment of an extra-bundle matrix octet. The section of emerging bundles (tangent or perpendicular to surface) is slightly undulating. Indeed, if edges of initially square section of bundles are emerging, creating crenels, they are smoothed out to a wavy form by ablation. A BM photograph of the surface and an OM micrograph of a polished slice, presented on Fig. 2-a and b, associated to the knowledge of the material structure, enable us to sketch the "pallet" scheme.

2. *Epimesostructural* roughness develops at the end of emerging bundles, and looks like "needle clusters" (resp. "needle layers") for bundles perpendicular (resp. parallel) to material surface. In the literature, many micrographs show such roughness features on carbon-based composites during ablation by oxidation [CHO93, DUV97] or both oxidation and sublimation. [CHO01, HAN95, LEE04] As shown on photographs 2-c and d, due to an important recession of the intra-bundle matrix, fibers, which are less reactive, are partially stripped, become thinner, and acquire a needle shape.

3. *Epmicrostructural* roughness appears on the microstructure. Fiber tips are faceted (Fig. 2-f). Moreover, Fig. 2-c and e also show holes on the top of the fibers.

From the above presented description and classification, it appears that ablation-related geometrical features of the rough surface mainly follow the material structure. Accordingly, it will be called *structural roughness* to make a difference with a purely *physical roughness* which has already been observed on homogeneous materials and modelled [DUF05]. This physical roughness consists in scalloped morphologies (regmaglypts) and is not correlated to material structure [VIG05]. The cause seems to be a dynamical effect based on the concurrence between bulk transfer and heterogeneous transfer, be it of mass or heat. In addition to such a competition, possible physical phenomena leading to structural roughness appear to be reactivity differences between phases. As a result, models including structure and physics have to be taken in consideration.

2. MODEL SETUP

The starting point for a model for ablation is the Hamilton-Jacobi equation for the recession of a surface defined by the relation $S(x,y,z,t) = 0$:

$$\frac{\partial S}{\partial t} + \mathbf{v} \cdot \nabla S = 0 \quad [1]$$

where the expression for surface recession velocity [DUF05] is :

$$\mathbf{v} = -v_s R \mathbf{n} \quad [2]$$

Here, $v_s = M_s/\rho_s$ is the solid molar volume, $\mathbf{n} = \frac{\nabla S}{||\nabla S||}$ the normal pointing outwards of the surface, and R is the molar rate of ablation, which is itself expressed as a function of temperature and reactant gas concentration [DUF05]:

$$R = k(T) f(C,T) \quad [3]$$

In the case of oxidation, the reactant gas is the oxidative species and one has $f(C) = C^\alpha$ (α is a reaction order) and in the case of sublimation, the considered gas is gaseous carbon and one has $f(C) = (C_{eq}(T) - C)$ [DUF05]. Note that $k(T)$ is a quantity that is linked to the material : its variations from one constituent to another will be responsible for structural roughness. It is a well-known fact that the precise degree of organisation and density of a given carbon-based material influences strongly its heterogeneous chemical reactivity [DUV97, NAG62] as well as its sublimation rate [HAV02].

The description of roughness acquisition involves the evaluation of \mathbf{v} at any point of the interface, and this requires knowledge of the temperature T and concentration C fields, i.e. it is a non-local model. This latter requirement implies the resolution of balance equations for at least these two variables, where terms describing convection, diffusion, and consumption/creation may be included. The main point is that bulk transport and

heterogeneous consumption are possibly in concurrence, and it is anticipated that this competition may have strong effects on the surface geometry.

Various levels of modelling may be produced, depending on the choice of simplifications in the description of heat and mass balances. Very rich models have been produced for the description of the gas phase in ablation systems [COU98,KEE93,ROB94], but none have included the coupling with a Hamilton-Jacobi recession equation. In this work, the models used are very simple, but they allow to emphasise on transfer competition.

The simplest model is isothermal, and features only diffusion of the considered gaseous species, in competition with heterogeneous consumption. It is of interest at those scales where temperature gradients are negligible, *i.e.* below 0.1 mm in length perpendicular to the average surface in application-like experiments, or at any scale in isothermal conditions (oxidation reactor). The basis set of equations, derived in [DUF05], is :

$$\left\{ \begin{array}{l} \frac{\partial S}{\partial t} + \mathbf{v} \cdot \nabla S = 0 \\ \mathbf{v} = -v_s R \mathbf{n} \\ R = kC \quad \text{at } S(x, y, z, t) = 0 \\ \nabla \cdot (-D \nabla C) = 0 \quad \text{at } S(x, y, z, t) \geq 0 \\ -D \nabla C \cdot \mathbf{n} = -R \quad \text{at } S(x, y, z, t) = 0 \end{array} \right. \quad [4]$$

Note that diffusion is considered as steady-state, because the characteristic time for gas concentration instationarity is much shorter than for surface recession.

For large scales, heat transfer has to be accounted for ; but now it is the concentration field that becomes a simple constant, because of the relatively small consumption rate. So another model featuring only a heat balance equation may be set up. In a first modelling attempt, convection and radiation will be discarded ; removing such strong hypotheses will be the subject of future work. The model equations are then :

$$\left\{ \begin{array}{l} \frac{\partial S}{\partial t} + \mathbf{v} \cdot \nabla S = 0 \\ \mathbf{v} = -v_s R \mathbf{n} \\ R = k_0 C_0 \exp\left(-\frac{E_a}{\mathfrak{RT}}\right) \quad \text{at } S(x, y, z, t) = 0 \\ \nabla \cdot (-\lambda_g \nabla T) = 0 \quad \text{at } S(x, y, z, t) \geq 0 \\ \nabla \cdot (-\lambda_s \nabla T) = 0 \quad \text{at } S(x, y, z, t) \leq 0 \\ -[\lambda \nabla T]_{g \rightarrow s} \cdot \mathbf{n} = -L_r R \quad \text{at } S(x, y, z, t) = 0 \end{array} \right. \quad [5]$$

where λ_g and λ_s are the respective heat conductivities of the gas and solid and L_r is the reaction molar enthalpy and the term between square brackets is the interfacial heat flux jump. One notes the large similarity between this model and the preceding one, the difference being that conduction inside the solid phase has to be accounted for.

In addition to these specifications, one has to provide a resolution domain, which is intended to describe “enough material” and “enough fluid over it”. In practice, periodicity in the average normal direction will be used, and the fluid height will be chosen so that the concentration or temperature field at the top of the simulation box ($z = \delta_n$) becomes flat, *i.e.*, the box top lies higher than the characteristic dimension of the perturbations introduced by ablation on the scalar fields C or T . An elementary perturbation analysis performed on the diffusion or conduction equation shows that the characteristic decay length of a perturbation of C or T is of the same order of magnitude as the spatial period of the material heterogeneity, so three times the size of the transversely periodic unit cell is a good rule of thumb.

Equations [4] have been solved by two independent numerical methods, one based on a Monte-Carlo Random Walk algorithm for diffusion and a simplified marching-cube description of the moving surface [LAC06], the other one based on a Finite Volume discretisation for diffusion and a VOF (Volume-Of-Fluid) method with PLIC (PLanar Interface Construction) discretisation for the surface [ASP05] ; both were validated against each other and against analytical solutions for the recession of a flat homogeneous interface.

3. RESULTS

3.1 Fibre-scale results

The first application case for the modelling strategy is the epimesostructural roughness. It is clearly a structural roughness linked to the reactivity difference between the fibre and the surrounding matrix or interphase. Fig. 3 is an illustration of the resolution domain and boundary conditions for a fibre-scale isothermal ablation problem. If the value of the gas diffusion coefficient is easy to estimate, it is not the case for the heterogeneous reactivity of the constituents ; thus, a parameter variation study has been performed.

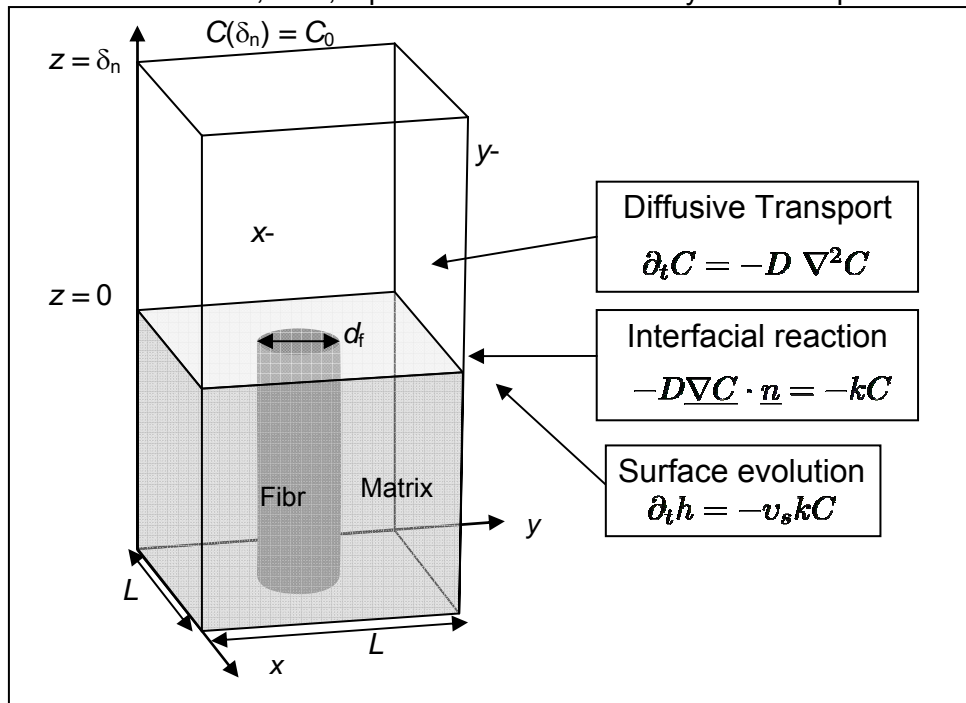


Figure 3 : Resolution domain and boundary conditions for an isothermal fibre-scale ablation problem. For $t > 0$, the simulation cell is translated so that $z=0$ always coincides with the highest solid point.

All numerical computations yielded a transient behaviour during which roughness increases from the initial flat surface, and eventually a steady state, *i.e.* a recessing surface with a preserved geometry, typically a needle-shaped fibre emerging from a nearly flat matrix bottom.

The influence of three dimensionless groups on the stationary roughness profiles of "needle clusters" has been identified :

- ° A geometrical parameter : $\tilde{r}_f = r_f/L$, with r_f : fiber radius, and L : square base unit cell size. Note that it is directly related to the fiber volume fraction $V_f = \pi \tilde{r}_f^2$

- ° A Sherwood number for the fiber : $Sh_f = k_f r_f / D$, which translates the diffusion/reaction competition,

- ° A matrix/fibre reactivity ratio : $\tilde{k} = k_m / k_f$

The model sensitivity to each one of these three dimensionless groups is tested from a central case ($Sh_f = 0.03$, $\tilde{k} = 10$, $\tilde{r}_f = 0.3$) and is summarized at fig. 4. For each simulation case, the steady state regime is reached after a computing time ranging from 1 to 24 hours with a Xenon CPU 3.2GHz processor. Let us describe the morphological evolutions of roughness features as the dimensionless groups are varying. Peak-to-valley roughness increases together with:

- ° the fiber/cell ratio (\tilde{r}_f) in an almost homothetic way;
- ° the inverse of the Sherwood number (Sh_f) from a flat to an almost pyramidal geometry;
- ° Reactivity ratio (\tilde{k}) from a flat to a needle-like geometry.

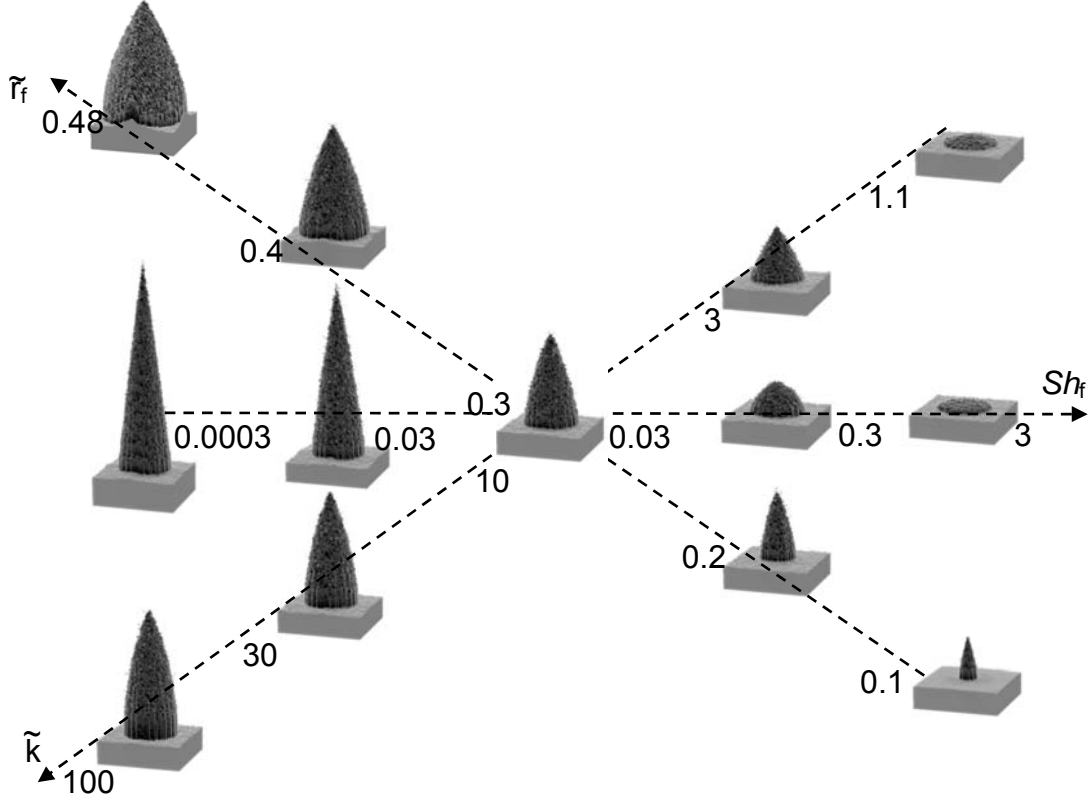


Figure 4: Parametric study at mesoscopic scale

Limiting cases are observed. On the right side of fig. 4, roughness set-up becomes impossible, since the problem turns out to be 1-D for at least one of these reasons (from top to bottom): (i) the solid becomes chemically homogeneous ($\tilde{k} \rightarrow 1$); (ii) diffusive limitation ($Sh_f \rightarrow \infty$); (iii) the solid becomes single-phased ($\tilde{r}_f \rightarrow 0$). On the left side, the peak-to-valley roughness is maximal since (from top to bottom): (i) fiber diameter is maximal ($\tilde{r}_f \rightarrow 1$), (ii) reactive limitation on fiber and matrix is reached ($Sh_f \rightarrow 0$), (iii) difusive limitation on matrix is reached ($\tilde{k} \rightarrow \infty$).

As a result, it is possible to analyze real morphologies through those first results. Of course, the simplicity of the model used has to be kept in mind. A comparison of Fig. 4 to micrographs of Fig. 2-d and f tends to show that the actual material reactivity ratio between fibre and matrix is high, and that the chemical etching of the fibre is slow with respect to diffusion.

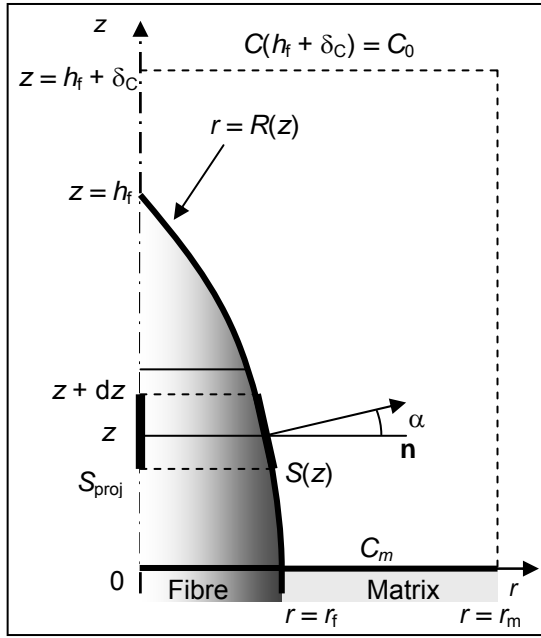


Figure 5: Axisymmetrical simplification for the isothermal fibre-scale ablation problem at steady-state

The dependency of the steady morphologies on the three dimensionless parameters has been more rigorously demonstrated in the frame of an analytical resolution, considering a cylindrical system with one central fibre and a matrix ring around it, as illustrated at figure 5. It is easy to relate the lateral and vertical recession velocities to the local slope :

$$dR(z) = - C(z) k_f v_f (V_z \cos \alpha)^{-1} dz \quad [6]$$

The slope term $(\cos \alpha)^{-1}$ is $(1 + (dR/dz)^2)^{1/2}$ and the global velocity is evaluated at the matrix position :

$$V_z = C(0) k_m v_m \quad [7]$$

If there is a steady state for the surface, then the diffusive gas flux is purely vertical. This allows to write down the following relation :

$$C(z) = C(0) + (C(h_f) - C(0)) \cdot (z/h_f) \quad [8]$$

Combining all these relations together gives a differential equation describing analytically the fiber tip :

$$\frac{dR}{dz} = - \frac{1 + (z/La)}{\sqrt{A^2 + (1 + (z/La))^2}} ; \quad R(z=0) = r_f \quad [9]$$

with $A = \tilde{k} (v_m/v_f)$ and $La = D/k_m = \frac{r_f}{\tilde{k} S h_f}$. Integration of eqs. [9] for z from 0 to h_f ,

subject to the condition that $\frac{r_f}{La} < \sqrt{A^2 - 1}$, allows to give an expression for the peak-to-valley roughness :

$$h_f = r_f \left(\tilde{k} S h_f \right)^{-1} \left(\sqrt{\left(\tilde{k} S h_f \right)^2 + 2\sqrt{A^2 - 1} \left(\tilde{k} S h_f \right)} + 1 - 1 \right) \quad [10]$$

The tendencies described from the numerical study are indeed contained in eq [10]. The transient time, that is, the time period before the surface morphology gets steady, has been found numerically to obey the following law :

$$\tau \sim 3 \frac{(\delta_c + h_f)^2}{D C_b v_m} \quad [11]$$

Where δ_c is the diffusive boundary layer thickness and C_b the reactant gas concentration in the bulk. Note that δ_c may not be equal to the numerical parameter δ_n .

The overall recession velocity in steady state is :

$$V_z = C_b k_m v_m (1 + k_m (h_f + \delta_c)/D)^{-1} \quad [12]$$

This relation – also well verified by the numerical computations -- provides a “composite law” where it is seen that a simple mixture rule is not sufficient to correctly

describe the material behavior. Equivalent reactivity and molar volume may be given, in order to use them at a superior scale :

$$v_{\text{eff}}^{-1} = V_f v_f^{-1} + (1 - V_f) v_m^{-1} \quad [13]$$

$$k_{\text{eff}} = v_{\text{eff}}^{-1} k_m v_m (1 + h_f/La + (1 - v_m/v_{\text{eff}}) \delta_c/La)^{-1} \quad [14]$$

Note that the effective constant is a function of the diffusive boundary layer thickness when there is a contrast in molar volumes (*i.e.* in densities) between fibre and matrix. From the definition of La , it is seen in eq. [14] that the matrix reactivity is the most determining parameter for the effective behaviour : it is a “weakest link law” that appears from this analysis.

Using relations [10] and [14] provides a means to perform identifications of the fiber and matrix reactivities, from the experimental values of the peak-to-valley roughness h_f and of the overall recession velocity V_z .

3.2 Bundle-scale results

The second scale considered here is the macrostructure. For sake of simplicity, the samples resulting from oxidation have been simulated first, because it is possible to keep on using eqs [4], using now an average reactivity for the bundle.

A numerical unit cell has been designed as sketched at figure 6a ; the steady state morphology is presented at figure 6b ; its similarity with figure 2b supports the conclusion that the model is adequate ; again, it allows possible to identify matrix and bundle effective reactivities from the peak-to valley roughness or some other geometrical parameter and the overall steady recession velocity.

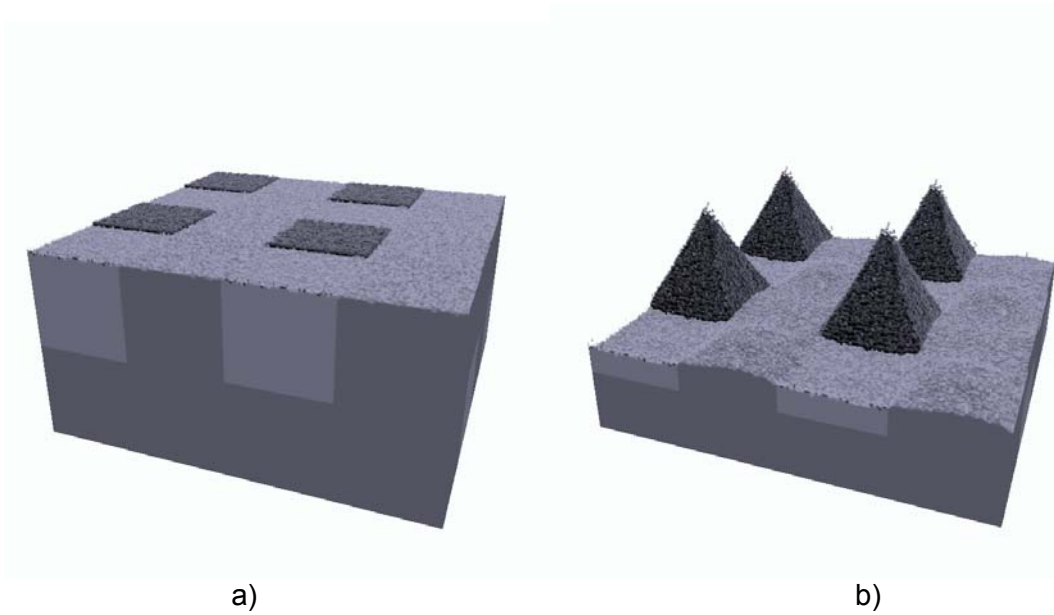


Fig. 7 : 3D composite material macro scale ablation simulations : a) at $t = 0$, b) at $t = 3\tau$

When the material is ablated in thermal gradient conditions, one has to substitute eqs [5] to eqs. [4] ; however, the temperature plays the same role as gas concentration, the gas thermal diffusivity $a_g = \lambda_g / \rho_g C_{pg}$ is analogous to the mass diffusivity D , and the reactivity k has to be replaced by an equivalent group. If T_0 is a reference temperature associated to the surface, then a linearization of eqs [5] allows to identify this group as :

$$K = (L_r/C_{pg} T_0)(E_a/R T_0)k(T_0) \quad [15]$$

where C_{pg} is the molar heat capacity of the gas. This turns the thermal-based problem equivalent to the preceding one, at the exception that the temperature distribution in the solid phases is not flat nor 1D in general case. Numerical developments to treat this model are currently under way. It is already interesting to note that if a and D are generally of the same

order of magnitude in a gas, parameter k' may be much larger than k , because the activation energy may be high as well as the reaction or sublimation molar enthalpy change. Indeed, in the case of physical roughening of homogeneous surfaces [DUF05], it has been verified that the thermal-driven roughness scale is much larger than the mass transfer-driven one.

4. Conclusion

In this work, the origin and development of roughness on a 3D-C/C ablative composite during atmospheric crossing are tackled. First, using as references arc-jet test and oxidation test samples, multi-scale roughness is observed, classified and briefly analyzed as a whole. An analysis of the roughness causes brings the production of simple bulk transfer/interface transfer models concerning either mass or heat. In the case of mass transfer, the use of efficient homemade 3D numerical simulation codes enabled to perform simulations at fibre scale and bundle scale. The obtained morphologies are coherent with the observations on samples. The influence of some parameters, like reactivity contrast, diffusion-to-reaction ratio, and fibre volume fraction, on peak-to-valley roughness depth has been recognized and confirmed by an analytical study at fibre scale. The average composite reactivity is shown to depend mostly on the weakest component's reactivity, and on the roughness itself. This study opens the possibility to determine, by inverse analysis, either mass transfer properties or material intrinsic reactivities.

The presented model based on heat transfer are currently under numerical investigation, however, some analogies are pointed out, suggesting that the experience on mass-transfer models will be easily adapted to heat this case.

Future directions in this work are : (i) an exploitation of the presented method on other materials and conditions, (ii) the consideration of heat transfer, either alone, or coupled to mass transfer, (iii) the incorporation of convection to the models.

Acknowledgements

Financial support through Ph.D. grants from CEA to J. L. and from Snecma Propulsion Solide to Y. A. is acknowledged. The authors are also indebted to G. Duffa, J.-M. Goyhénèche, J.-F. Epherre (CEA), C. Descamps and F. Plazanet (SPS) and M. Quintard (CNRS-IMFT) for fruitful discussions.

References

- [MAN98] L. M. Manocha and E. Fitzer. Carbon reinforcement and C/C composites. Springer, Berlin (1998).
- [DUF96] G. Duffa, Ablation. CEA, Le Barp, France ISBN 2-7272-0207-5 (1996)
- [SAV93] G. Savage, Carbon/Carbon Composites. Chapman & Hall, London (1993)
- [COU98] J. Couzi, J. de Winne, and B. Leroy. Improvements in ablation predictions for reentry vehicle nosetip. In Proc. 3rd European Symp. on Aerothermodynamics for Space Vehicles, pp. 493—499, ESA, Noordwijk, The Netherlands (1998).
- [JAC74] M. D. Jackson. Roughness induced transition on blunt axisymmetric bodies, Interim Report SAMSO-TR-74-86 of Passive Nosetip Technology (PANT) Program n°15 (1974).
- [RED79] D. C. Reda. Correlation of nosetip boundary-layer transition data measured in ballistic-range experiments, Sandia Report SAND 79-0649 (1979).
- [BAT83] R. G. Batt and H. H. Legner. A review of roughness-induced nosetip transition, AIAA Papers 21, 7-22 (1983).
- [BOR90] V. Borie, Y. MAisonneuve, D. Lambert and G. Lengellé. Ablation des matériaux de tuyères de propulseurs à propergol solide. Technical Report N°13, ONERA (1990)
- [WOO75] M. R. Wool. Summary of experimental and analytical results, Interim Report SAMSO-TR-74-86 of Passive Nosetip Technology (PANT) Program n°10 (1975).
- [CHO93] D. Cho, J. Y. Lee, and B. I. Yoon. Microscopic observations of the ablation behaviours of carbon fibre/phenolic composites. J. Mater. Sci. 12:1894-1896 (1993).
- [DUV97] E. Duvivier. Cin'etique d'oxydation d'un composite carbone/carbone et influence sur le comportement m'ecanique. PhD thesis n° 1692, University Bordeaux 1 (1997).

- [CHO01] D. Cho and B. I. Yoon. Microstructural interpretation of the effect of various matrices on the ablation properties of carbon-fiber-reinforced composites. *Compos. Sci. and Technol.*, 61:271-280 (2001).
- [HAN95] J. C. Han, X. D. He, and S. Y. Du. Oxidation and ablation of 3D carbon-carbon composite at up to 3000 °C. *Carbon* 33:473-478 (1995).
- [LEE04] Y.-J. Lee and H. J. Joo. Investigation on ablation behavior of CFRC composites prepared at different pressures. *Composites: Part A* 35:1285-1290 (2004).
- [VIG05] G. L. Vignoles, J.-M. Goyheneche, G. Duffa, T.-H. N'guyen-Bui, A. Velghe, B. Dubroca and Y. Aspa. Scalloped morphologies of ablated materials, *Ceram. Eng. Sci. Proc.* 26(2): 245 (2005).
- [DUF05] G. Duffa, G. L. Vignoles, J.-M. Goyhénèche and Y. Aspa. Ablation of carbon-based materials : investigation of roughness set-up from heterogeneous reactions. *Int. J. of Heat and Mass Transfer*, 48:3387 (2005).
- [HAV02] M. A. Havstad and R. M. Ferencz. Comparison of surface chemical kinetic models for ablative reentry of graphite. *J. Thermophysics and Heat Transfer* 16:508 (2002).
- [NAG62] J. Nagle and R. F. Strickland-Constable. Oxidation of carbon between 1000-2000 # C. In Proceedings of 5th conference on carbon, p. 154 (1962).
- [KEE93] J. A. Keenan and G. V. Candler. Simulation of ablation in earth atmospheric entry. *AIAA Papers* 93 (1993).
- [ROB94] T. P. Roberts. Modelling gas/surface interaction processes of ablating wall boundaries associated with planetary entry. In Proc. 2nd European Symp. on Aerothermodynamics for Space Vehicles, p. 311, ESA, Noordwijk, The Netherlands (1994).
- [LAC06] J. Lachaud, G. L. Vignoles, J.-M. Goyheneche and J.-F. Epherre. Ablation in carbon/carbon composites : microscopic observations and 3D numerical simulation of surface roughness evolution, 6th Pacific Rim Conf. on Ceramic and Glass Technology (PacRim6), Maui, Hawaii, Sept. 2005 (to appear in *Ceram. Eng. Sci. Proc.*) (2006)
- [ASP05] Y. Aspa, M. Quintard, F. Plazanet, C. Descamps and G. L. Vignoles. Ablation of Carbon/Carbon Composites : Direct Numerical Simulation and Effective Behavior, *Ceram. Eng. Sci. Proc.* 26(2): 99 (2005).